The π, π^* State in Formaldehyde and Thioformaldehyde

F. GREIN AND M. R. J. HACHEY

Department of Chemistry, University of New Brunswick, Bag Service #45222, Fredericton, New Brunswick, Canada E3B 6E2; e-mail (F.G.): fritz@unb.ca

Received March 26, 1996; revised manuscript received June 11, 1996; accepted June 13, 1996

ABSTRACT

For formaldehyde, the C — O stretch potential of $^1(\pi, \pi^*)$ crosses all $^1A_1$ Rydberg potentials, such as $n, 3p_y$, $n, 3d_{yz}$, etc., thereby transferring the intensity of the unassigned $^1(\pi, \pi^*) \leftarrow \tilde{X}$ system to these Rydberg states. For thioformaldehyde, the situation is similar but a shift in the potentials allows for direct observation of $^1(\pi, \pi^*)$. In its $^1(\pi, \pi^*)$ state, H_2CO is planar, having a low barrier of about 0.2 eV toward the nonplanar $^1(\sigma, \pi^*)$ state. For H_2CS, the planar conformation of $^1(\pi, \pi^*)$ is a saddle point, with $^1(\sigma, \pi^*)$ being the global minimum on the $2^1A'$ surface. The triplet π, π^* states of H_2CO and H_2CS are nonplanar, having inversion barriers of 0.1 and 0.05 eV, respectively. For both H_2CO and H_2CS, the π, π^* configuration also crosses the ground-state configuration, which explains predissociation and radiationless transitions of some Rydberg states.

Introduction

In the absorption spectrum of formaldehyde, the electric dipole forbidden transition $^1A_2(n, \pi^*) \leftarrow \tilde{X}^1A_1$ is observed and well studied, whereas the allowed transition $^1(\pi, \pi^*) \leftarrow \tilde{X}^1A_1$, despite being predicted to be very intense, has so far escaped all attempts at detection. The problem of the "missing" $^1(\pi, \pi^*)$ state also plagues many other aldehyde and ketones. Consequently, Robin, a prominent reviewer in the field of higher excited states, wrote that "aldehydes and ketones are a most perplexing chromophoric group" [11].

For a long time, it was believed that $^1(\pi, \pi^*)$ had a vertical excitation energy in excess of the first ionization potential (IP) of 10.8887 eV [2] and, therefore, is not observed. For example, Langhoff et al. [3] predicted $^1(\pi, \pi^*)$ to be near 11.2 eV.

The absorption spectrum in the vacuum ultraviolet (VUV) region of formaldehyde was first studied by Price [4]. Currently, all medium and strong bands in the VUV spectrum of H_2CO are assigned to Rydberg transitions. The latest assignments by Brint et al. [5] identified $n \rightarrow s, p, d, f$-Rydberg transitions up to $5s$, $12p$, $12d$, and $9f$, converging to the first IP. However, in many cases, the intensities or quantum defects do not conform to expectations for Rydberg transitions. For example, the

International Journal of Quantum Chemistry: Quantum Chemistry Symposium 30, 1661–1671 (1996)

CCC 0360-8832 / 96 / 071661-11

intensity of $n,4p$ is higher than that of $n,3p$, and the quantum defect of $n,3d$ is 0.4, whereas it is expected to be ≤ 0.1. Further, for $n > 4$, the *np*, *nd*, and *nf* transitions have similar intensities, contrary to their normal behavior [1, 5]. Although the source of the Rydberg anomalies is usually attributed to Rydberg–valence interactions, the nature of the perturbing valence state has never been positively identified.

In contrast to the missing singlet $\pi \rightarrow \pi^*$ system, the triplet $\pi \rightarrow \pi^*$ system of H_2CO has been observed by electron impact studies ([6] and references therein). It should also be noted that the absorption spectrum of thioformaldehyde, whose electronic spectrum is expected to be similar to that of formaldehyde, shows a progression of bands, lying between $n \rightarrow 4s$ and $n \rightarrow 4p$, that were assigned to $^1(\pi, \pi^*)$.

Obviously, it is of significant interest to investigate theoretically the reasons for the strange behavior of the π, π^* state. In a series of multireference (MR) configuration interaction (CI) studies performed over the last few years, potential energy curves for the C — O stretch and the out-of-plane motion were obtained for H_2CO [7–11] and H_2CS [12–15]. Using more extended basis sets and large CI expansions, the vertical excitation energy of the $^1(\pi, \pi^*)$ state of H_2CO is calculated to be 9.6 eV [8]. It is important to include the doubly excited configuration n^0, π^{*2} in the set of reference configurations. From the calculated potential energies, vibronic energy levels and oscillator strengths were evaluated [8, 13]. The results, as they concern the π, π^* state of H_2CO and H_2CS, are most interesting and, in our opinion, explain why $^1(\pi, \pi^*)$ had previously not been assigned in the absorption spectrum of H_2CO.

Methods

Ab initio MR–CI calculations were performed using the MRD–CI programs [16]. A $(10s6p/5s4p)$ basis set for C and O, $(12s9p/5s4p)$ for S, with additional polarization functions and *s*, *p*, *d* Rydberg functions on C and O (C and S for H_2CS) is used. The hydrogen basis is $(5s/3s)$ with a *p* polarization function. Details are given in [8, 10, 13, 14]. In their ground states, H_2CO and H_2CS are planar, having C_{2v} symmetry. For the out-of-plane motion, C_s symmetry was observed. The number of reference configurations varied between 40 and 60. They were selected such that all symmetry-adapted functions (SAF) with $c^2 > 0.001$ in the final wave function were part of the reference space, for the whole range of geometries covered by the calculations.

The Role of $^1(\pi, \pi^*)$ in the Absorption Spectrum of H_2CO

In Figure 1, the $^1A_1$ potential curves for the C — O stretch of H_2CO are shown. They are similar to the ones obtained in [8], but a lower configuration selection threshold (4 μHartrees) was used. The other geometry parameters were held at experimental ground state (GS) values (R_{CH} = 2.0796 a_0 and ϕ(HCH) = 116.3° [17]). It is seen that diabatically the $^1(\pi, \pi^*)$ state crosses all Rydberg potentials, also the higher ones not shown here. Even the apparent long-distance minimum of $^1(\pi, \pi^*)$, at 2.914 a_0 is due to an avoided crossing of π, π^* with the GS configuration n^2. At 3 a_0, the 1^1A_1 wave function contains about 45% n^2 and 45% π, π^*, whereas 2^1A_1 has 40% n^2 and 45% π, π^* (see Fig. 2). (The percentage contribution was calculated from c_i^2, where c_i is the coefficient of the respective SAF in the CI wave function. In the CI expansion, $^1(n, \pi^*)$ MOs were used. The given numbers change slightly, but not greatly, with the choice of MOs.) At the largest CO distance shown in Figure 2, 4 a_0, the eventual dissociation to CH_2 + O is not yet important. Open-shell configurations to describe the dissociation become dominant at larger distances than shown. The repulsive crossing of $^1(\pi, \pi^*)$ with all $^1A_1$ Rydberg states *and* the ground state leads to predissociation and radiationless transitions. According to Figure 1, the doubly excited $^1(n^0, \pi^{*2})$ state appears at about 10.2 eV, having a fairly shallow potential, and crossing π, π^* at small R and higher Rydberg states at larger R.

Figure 3 shows an enlarged version of the C — O stretch curves for 2^1A_1 to 4^1A_1, including vibrational energy levels for each of the minima. It should be noted that all minima, except for $n,3p_y$ and $n,3d_{yz}$, are caused by avoided crossings with π, π^*. These potential wells are bounded by π, π^* on the left, and by a Rydberg configuration on the right. A notation such as $\pi, \pi^*/n,3p_y$, used here to describe such potentials, should be obvious.

Assuming that all $^1A_1$ states are planar, and that the C — O stretch vibrations can be approximated

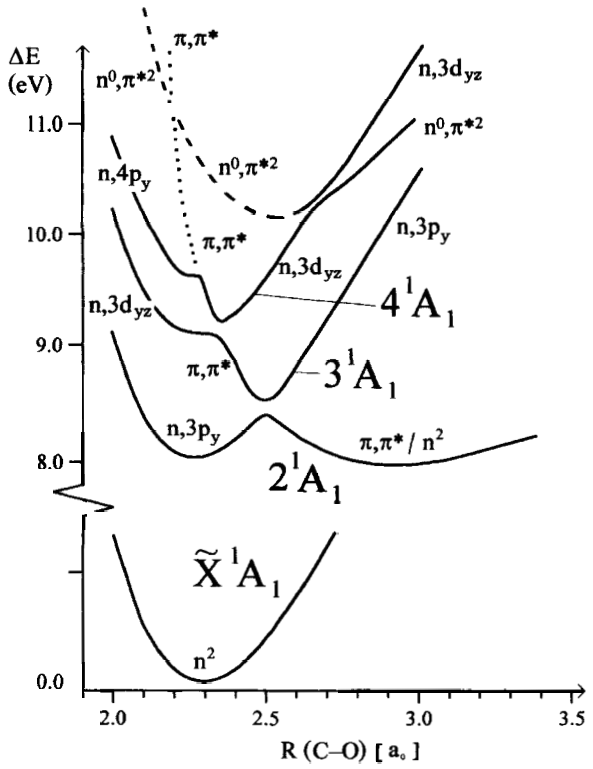

FIGURE 1. C — O stretch potentials for $^1A_1$ states of H_2CO.

by the one-dimensional potentials given in Figure 3, the vibronic oscillator strengths were evaluated for each vibrational level, by first calculating the electric dipole transition moment as a function of R_{CO} and then combining it with the Franck–Condon (FC) factor.

In Table I, experimental values for energies and oscillator strengths are compared with calculated vertical values and with vibronic values evaluated for each vibrational level, as described above. For the 0–0 bands of the $n \rightarrow 3s$ and $n \rightarrow 3p$ transitions, the vertical numbers agree reasonably well with the experimental values. However, for the 0–0 bands of $n \rightarrow 3d_{yz}$ (8.88 eV), $n,4s$ (9.26 eV), and higher states, the calculated vertical oscillator strengths are too small. Also, the 0–1 and 0–2 bands of Rydberg states have very low Franck–Condon factors, and the observed bands at 8.32, 9.04, and 9.18 eV could not be explained on the basis of vertical oscillator strengths.

In the last three columns of Table I, the calculated vibronic values are given. It is seen that vibronic energies can be matched with the energies of the observed bands to a maximum deviation of 0.24 eV, but mostly lying within 0.05 eV. Larger deviations may be indicative of the need for a non-Born–Oppenheimer treatment.

Except for the three lowest bands, the literature assignments, as given in Table I, had to be changed

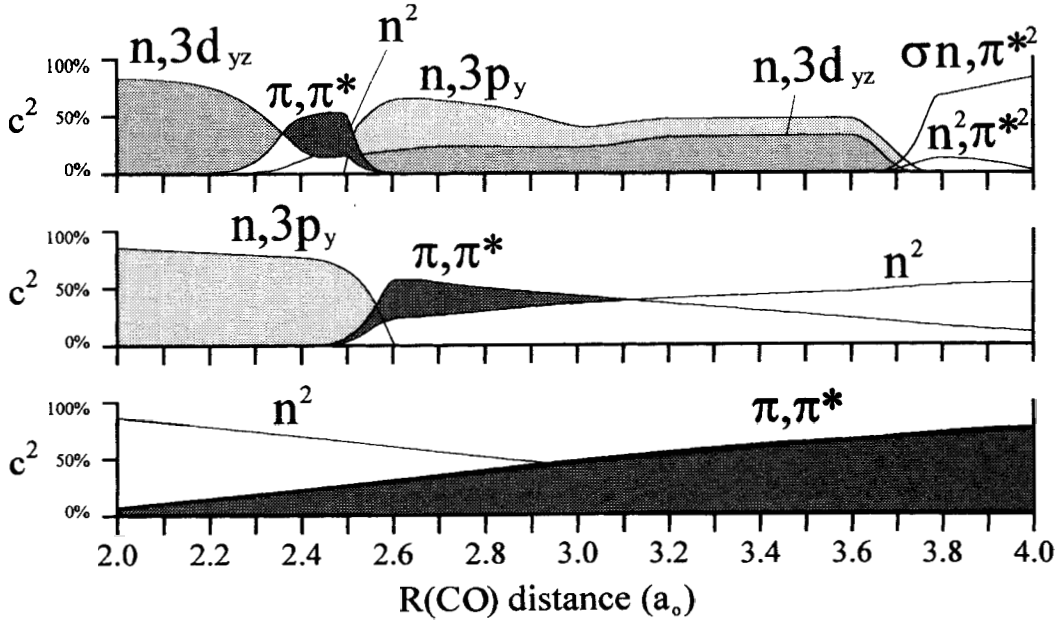

FIGURE 2. Contribution of various configurations to the wave functions 1^1A_1 to 3^1A_1 of H_2CO using $^1(n, \pi^*)$ molecular orbitals.

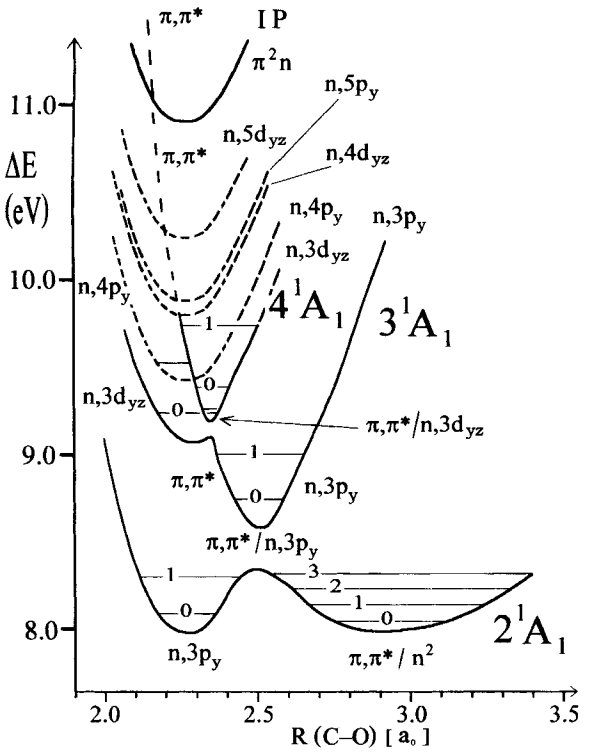

FIGURE 3. C — O stretch potentials for 2^1A_1 to 4^1A_1 states of H_2CO, showing vibrational energy as used in the calculations. Higher Rydberg potentials were estimated, and are shown as dashed lines.

to accommodate the new states that involve mixed π, π^*/Rydberg potentials. For example, the peak observed at 9.04 eV was originally assigned to the 3_0^1 band of $n, 3d_{yz}$, where ν_3 is the symmetric CH_2 bending vibration. By itself, $n, 3d_{yz}$ has low intensity. This band is now associated with 2_0^1 of $\pi, \pi^*/n, 3p_y$, where ν_2 is the C — O stretch vibration. It clearly derives its intensity ($f_{calc} = 0.024$, $f_{obs} = 0.022$) from the π, π^* section of the potential.

Most of the calculated oscillator strengths are in surprisingly good agreement with the observed values. Exceptions are the 0_0^0 band of $n, 3s$, for which vibronic interaction with $\sigma, \pi^*/\pi, \pi^*$ may play a role, as outlined in [7]. The small calculated f-value for the 8.32 eV band may be due to the fact that both the $v = 3$ level of $\pi, \pi^*/n^2$ and the $v = 1$ level of $n, 3p_y$ lie close to the barrier in the 2^1A_1 potential, which was not taken into account in the calculations. The third exception is the peak at 9.26 eV, for which f_{calc} is too large. It is presumed that the rapidly increasing density of states in this high-energy region may allow for other possible interpretations of the observed bands.

Overall, the results of Table I show that the π, π^* state is the major intensity provider for transitions to Rydberg states higher than $n, 3p$. Since intensities of Rydberg transitions normally decrease with increasing quantum number (as n^{-3} [3]), the contribution of π, π^* to Rydberg transitions beyond the ones covered here, such as $n, 4d$ and $n, 5s$, etc., should be even more significant,

TABLE I

Comparison of observed values for energies ΔE (in eV) and oscillator strengths f with calculated vertical and adiabatic values for bands of H_2CO lying above 7 eV.[a]

Experimental			Vertical		Vibronic		
ΔE	f	Assignment[b]	ΔE_{vert}	f_{vert}	ΔE	$f_0^{v'}$	Assignment[c]
7.09	0.033	$0_0^0\ n, 3s$	7.15	0.005	7.09	0.005	$0_0^0\ n, 3s$
7.97	0.018	$0_0^0\ n, 3p_z$	8.05	0.021	7.94	0.021	$0_0^0\ n, 3p_z$
8.12	0.035	$0_0^0\ n, 3p_y$	8.10	0.039	7.98	0.035	$0_0^0\ n, 3p_y$
8.32	0.005	$2_0^1\ n, 3p_y$	—	—	8.18	5×10^{-5}	$2_0^3\ \pi, \pi^*/n^2 + 2_0^1\ n, 3p_y$
8.88	0.014	$0_0^0\ n, 3d_{yz}$	9.25	0.005	8.64	0.012	$0_0^0\ \pi, \pi^*/n, 3p_y$
9.04	0.022	$3_0^1\ n, 3d_{yz}$	—	—	8.90	0.024	$2_0^1\ \pi, \pi^*/n, 3p_y$
9.18	~ 0.008	$3_0^2\ n, 3d_{yz}$	—	—	9.16	0.013	$2_0^2\ \pi/\pi^*/n, 3p_Y + 0_0^0\ n, 3d_{yz}$
9.26	~ 0.001	$0_0^0\ n, 4s$	9.19	6×10^{-5}	9.27	0.049	$0_0^0\ \pi, \pi^*/n, 3d_{yz}$
9.63	0.033	$0_0^0\ n, 4p_y$	9.41	9×10^{-5}	9.63	0.027	$2_0^1\ \pi, \pi^*/n, 3d_{yz}$
		$0_0^0\ n, 4p_z$	9.47	9×10^{-4}			

[a]Data taken from [8, 11] and experimental references therein, except for vertical oscillator strengths.
[b]Literature assignment where ν_2 is CO stretch and ν_3 is CH_2 symmetric bend.
[c]New assignments based in part on π, π^* / Rydberg potentials.

explaining the relatively high intensity observed for higher Rydberg states.

For other vibrational modes, the changes in geometry between the GS and excited Rydberg states are usually small (as tested in full geometry optimizations [10]), and, therefore, the 0–0 transition is expected to contain most of their intensity. Complications due to π,π^*, as encountered for the C — O stretch, are not likely.

Other symmetry species, such as $^1B_1$ $(n,3d_{xy};\ldots)$ and $^1B_2(n,3s;\ n,3p_z;\ n,3d_{x^2-y^2};$ $n,3d_{z^2};\ldots)$ are not affected by direct coupling with π,π^*. Therefore, C — O stretch bands of higher Rydberg states not belonging to the A_1 symmetry species cannot receive intensity from π,π^* directly and should therefore have much lower oscillator strengths than those of the $^1A_1$ transitions.

This is borne out by the vertical oscillator strengths given in Table I for $n,4s$ and $n,4p$ ($\sim 10^{-4}$). The calculated (vertical) oscillator strengths for $n,3d_{x^2-y^2}$, $n,3d_{z^2}$, and $n,3d_{xy}$ are 0.001, 0.005, and 3×10^{-5}, respectively. Using T_e values of 9.12, 9.06, and 9.30 eV [8], respectively, these $3d$-Rydberg transitions may be hidden in the more intense bands observed at 9.04, 9.18, and 9.26 eV.

The Geometry of the $^1(\pi,\pi^*)$ State of H_2CO

In Figure 4, the out-of-plane potentials are shown for the $2^1A'$ and $3^1A'$ states of H_2CO at $R_{CO} = 2.914\ a_0$, corresponding to the $\pi,\pi^*/n^2$ minimum of 2^1A_1 (Fig. 1). R_{CH} and ϕ(HCH) were kept at the GS values. It is seen that $\pi,\pi^*/n^2$, at that distance about an equal mix of π,π^* and n^2, is planar, although there is only a small barrier of about 0.2 eV toward the nonplanar σ,π^*. In all out-of-plane conformations, π,π^* mixes with σ,π^*, and for $\theta = 42.1°$ and $R_{CO} = 2.89\ a_0$ (the minimum of σ,π^*), the $2^1A'$ wave function is 44% σ,π^*, 32% π,π^*, and 11% n^2.

Contour plots of $2^1A'$ are shown in Figure 5, and 3-dimensional plots, in Figure 6. The local π,π^* minimum is confined to a small range of coordinates, whereas $n,3p_y$ is more extended; in comparison, the global σ,π^* minimum covers a wide range of geometries. Optimized geometries and adiabatic excitation energies for $^1(\pi,\pi^*)$, $^1(\sigma,\pi^*)$, and $^1(n,3p_y)$, all lying on the $2^1A'$ surface, are given in Table II. The σ,π^* minimum lies about 0.35 eV below the π,π^* minimum.

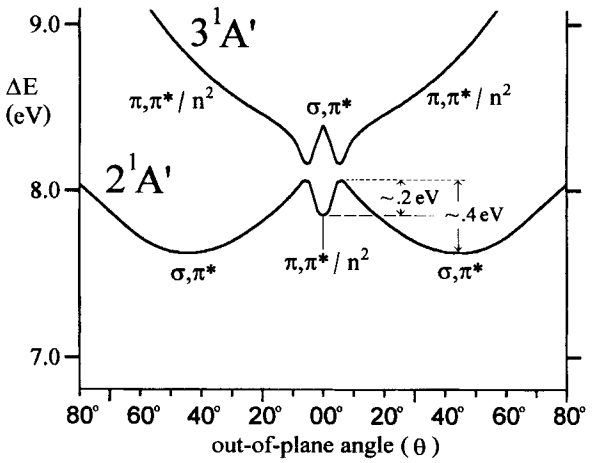

FIGURE 4. Out-of-plane potentials for $2^1A'$ and $3^1A'$ of H_2CO, at $R_{CO} = 2.914\ a_0$.

The low barrier of π,π^* toward σ,π^* implies that the higher vibrational levels of the $\pi,\pi^*/n^2$ minimum in Figure 3 are not bound by $\pi,\pi^*/n^2$ but only by σ,π^*. Therefore, for such higher levels, the C — O mode may mix with the out-of-plane mode.

The $^1(\pi,\pi^*)$ State of H_2CS

In Figure 7, the C — S stretch potentials of the $^1A_1$ states of H_2CS are given. The R_{CH} distance and ϕ(HCH) angles were kept at the experimental values of 2.0645 a_0 and 116.87° [18]. As in the case of H_2CO, π,π^* crosses all Rydberg states. However, there is an important difference. The crossing of the lowest A_1 Rydberg state $n,4p_y$ occurs near its minimum rather than at larger R, as was the case in H_2CO. Therefore, the potential well for $n,4p_y$ has effectively disappeared. The left-side turning points for the vibrational levels of the π,π^* potential move closer to the GS equilibrium distance, making the Franck–Condon factors for the electronic transition to π,π^* more favorable.

As for H_2CO, the 2^1A_1 wave function has an increasing contribution from n^2 as R_{CS} increases. At 3.85 a_0, 2^1A_1 is 37% π,π^* and 42% n^2, whereas 1^1A_1 is 52% π,π^* and 36% n^2. The participation of the major configurations in the wave function is very similar to the case of H_2CO which was shown in Figure 2. Figure 7 also indicates that the doubly excited state n^0,π^{*2} has dropped below $n,3_{yz}$,

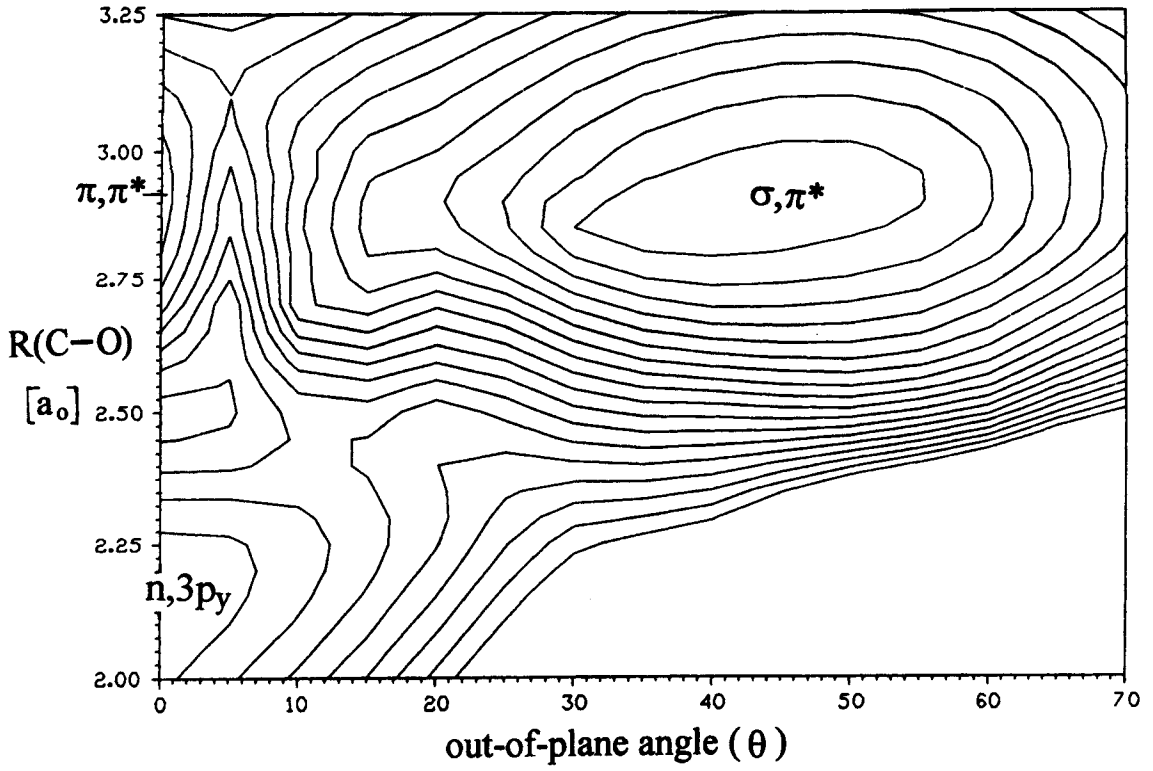

FIGURE 5. Contour plots for the $2^1A'$ state of H_2CO. R_{CO} distance in a_0 and angle θ in degrees. The outermost contour is 8.5 eV, and the innermost is 7.65 eV.

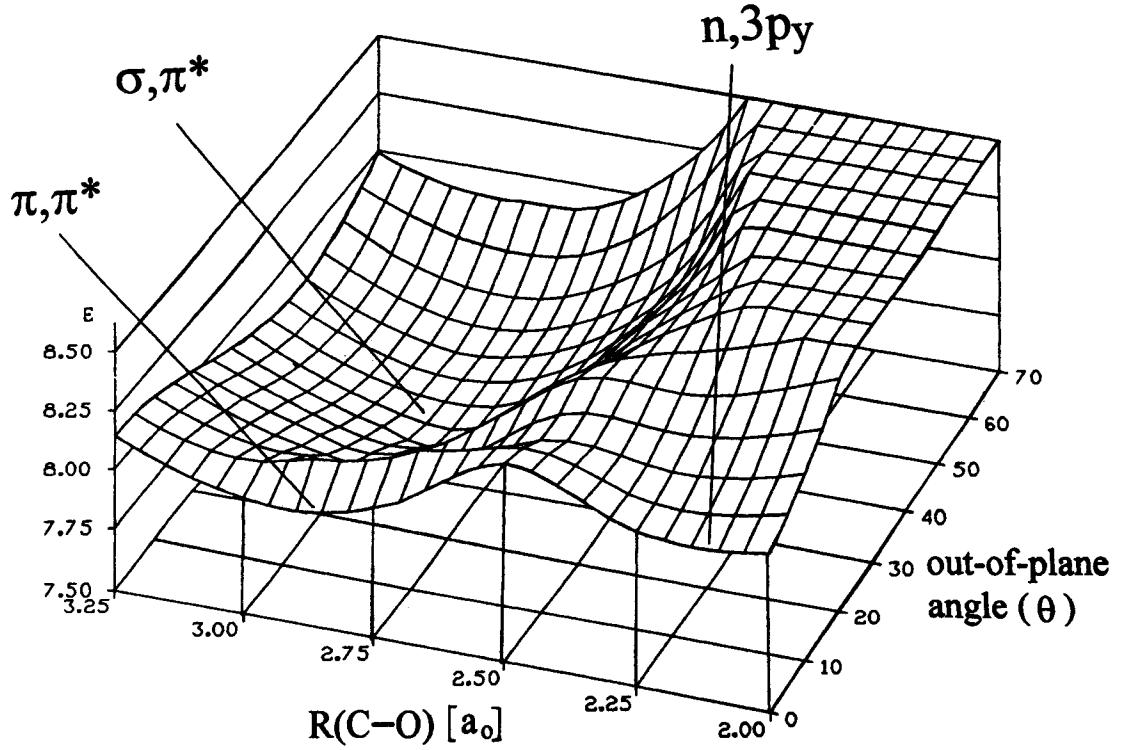

FIGURE 6. Three-dimensional plot of $2^1A'$ potential surface of H_2CO. Energies in eV relative to the ground state, R_{CO} distance in a_0 and angle θ in degrees.

TABLE II

Calculated and observed bands for H_2CO and optimized geometries for selected states of H_2CO.[a]

ΔE calcd. (exptl.)	ΔE_{vert}	$f_0^{v'}$ calcd. (exptl.)	f_{vert}	Assignment[a]
7.09 (7.09)	7.15 {7.30}	0.005 (0.033)	0.005 {0.006}	$0_0^0\ n, 3s$
7.94 (7.97)	8.05 {8.09}	0.021 (0.018)	0.021 {0.023}	$0_0^0\ n, 3p_z$
7.98 (8.12)	8.10 {8.12}	0.035 (0.035)	0.039 {0.041}	$0_0^0\ n, 3p_y$
8.15 (8.37)	8.32 {8.32}	— (—)	—	$0_0^0\ n, 3p_x$
8.18 (8.32)	— {7.30}	5×10^{-5} (5×10^{-3})	—	$2_0^1\ n, 3p_y \rightarrow$ $2_0^3\ \pi, \pi^*/n^2 + 2_0^1\ n, 3p_y$
8.64 (8.88)		0.012 (0.014)		$0_0^0\ n, 3d_{yz} \rightarrow$ $0_0^0\ \pi, \pi^*/n, 3p_y$
8.90 (9.04)	—	0.024 (0.022)	—	$3_0^1\ n, 3d_{yz} \rightarrow$ $2_0^1\ \pi, \pi^*/n, 3p_y$
9.16 (9.18)		0.013 (~ 0.008)		$3_0^2\ n, 3d_{yz} \rightarrow$ $2_0^2\ \pi, \pi^*/n, 3p_y + 0_0^0\ n, 3d_{yz}$
9.18	9.25 {9.24}		5×10^{-3} {3×10^{-3}}	$-\ n, 3d_{yz}$
9.10	9.80 {9.13}		1×10^{-3} {6×10^{-3}}	$-\ n, 3d_{x^2-y^2}$
9.06	9.37 {9.31}		5×10^{-3} {1×10^{-3}}	$-\ n, 3d_{z^2}$
9.17	9.40 {9.31}		—	$-\ n, 3d_{xz}$
9.30	9.34 {9.23}		3×10^{-5} {3×10^{-4}}	$-\ n, 3d_{xy}$
9.19		9×10^{-5}		$-\ n, 4s$
9.27 (9.26)		0.049 (~ 10^{-3})		$0_0^0\ n, 4s \rightarrow$ $0_0^0\ \pi, \pi^*/n, 3d_{yz}$
9.41		9×10^{-5}		$-\ n, 4p_y$
9.47		5×10^{-4}		$-\ n, 4p_z$
9.63 (9.63)		0.027 (0.033)		$0_0^0\ n, 4p \rightarrow$ $2_0^1\ \pi, \pi^*/n, 3d_{yz}$

Optimized geometries and T_e for selected states of H_2CO[b]

State	Configuration	R_e(CO) (a_0)	θ(OOP) (degrees)	ϕ(HCH) (degrees)	R_e(CH) (a_0)	T_e (eV)
2^1A_1	π, π^*	2.914	0.0	120.8	2.113	7.95
$2^1A'$	σ, π^*	2.890	42.1	115.1	2.040	7.59
2^1A_1	$n, 3p_y$	2.266	0.0	123.3	—	7.89
$1^3A'$	π, π^*	2.789	38.1	119.9	2.032	4.43
$2^3A'$	σ, π^*	2.750	35.5	133.5	2.060	7.15
2^3A_1	$n, 3p_y$	2.256	0.0	—	—	~ 7.89

[a] ν_2 is CO stretch and ν_3 is CH_2 symmetric bend.

[b] Optimized geometries obtained from [10] for the singlets and [9] for the triplets.

interfering with the π, π^* and $n, 3d_{yz}$ potentials at smaller R and with $n, 4p_y$ at larger R.

In Figure 8, the out-of-plane potential is shown for the $2^1A'$ state of H_2CS, at both $R_{CS} = 3.436\ a_0$ and $R_{CS} = 3.850\ a_0$. The latter distance corresponds to the C_{2v} minimum of π, π^*. At 3.436 a_0, π, π^* has a minimum with a low barrier toward σ, π^*. However, at the π, π^* equilibrium distance of 3.850 a_0, $2^1A'$ has a slight maximum at $\theta = 0°$. While π, π^* may still be called planar (the diabatic π, π^* potential is indicated by the dashed curve), the planar minimum is a *saddle* point in the 3-dimensional potential surface including the out-of-plane angle, rather than a local minimum.

In Table III, the optimized geometries of the $^1(\pi, \pi^*)$, $^1(\sigma, \pi^*)$, and $^1(n, 4p_y)$ states, all lying on the $2^1A'$ surface, are given, together with T_e values. It should be noted that the minimum of σ, π^* lies only 0.07 eV below that of π, π^*. Therefore, π, π^* (and σ, π^*) have a shallow potential both

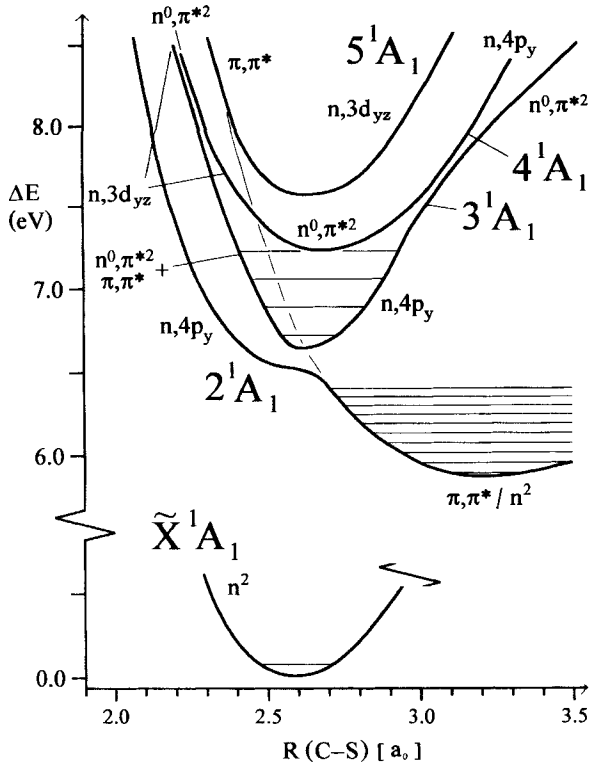

FIGURE 7. C — S stretch potentials for $^1A_1$ states of H_2CS.

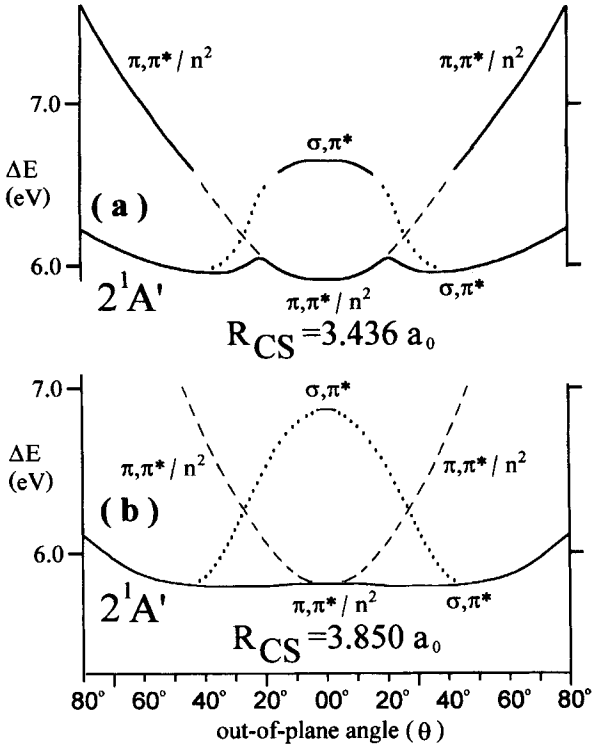

FIGURE 8. Out-of-plane potentials for $2^1A'$ state of H_2CS, at R_{CS} = 3.436 a_0 and at 3.850 a_0.

for the C — S stretch and the out-of-plane angle, constituting a shallow potential over two dimensions rather than just one. The implications for spectroscopy should be rather interesting.

As mentioned in the Introduction, the π, π^* spectrum of H_2CS is known, and the observed bands have been interpreted as belonging to the C — S stretch mode ν_3. For an out-of-plane angle of 36.2°, corresponding to the optimized value of $2^1A'$, the C — S potential is virtually parallel to the C — S potential for planar H_2CS (see dashed curve in Fig. 9). Therefore, the C — S stretch vibrational energies and vibronic oscillator strengths calculated in [13] for the supposedly planar π, π^* state, and reproduced in Table IV, retain some validity, although all energies should be corrected by the out-of-plane stabilization energy.

If the calculated energies are matched with nearest experimental values, as done in Table IV, then the problem arises that calculated oscillator strengths for the low-lying bands are too small to explain their observation. Therefore, a shift of the calculated energies toward the reported band origin at 5.54 eV is necessary. Also, a case has been made in [13] that hot bands, starting from $v'' = 1$ of the GS, might play a role. Since our calculated vibrational frequency of 473 cm^{-1} lies near the experimental value of 476 cm^{-1}, it should be possible, by proper choice of the origin and inclusion of hot bands, to match the experimentally observed spectrum quite closely.

TABLE III
Optimized geometries and T_e for selected states of H_2CS.[a,b]

State	Configuration	R_e(CO) (a_0)	θ(OOP) (degrees)	ϕ(HCH) (degrees)	T_e (eV)
2^1A_1	π, π^*	3.850	0.0	118.5	5.85
$2^1A'$	σ, π^*	3.672	36.2	112.5	5.78
2^1A_1	$n, 4p_y$	3.155	0.0	~ 122	6.63
$1^3A'$	π, π^*	3.483	28	119.8	2.70
$2^3A'$	σ, π^*	3.553	56	131.5	5.52
2^3A_1	$n, 4p_y$	3.024	0.0	120.9	6.49

[a] Optimized geometries obtained from [14] for the singlets and [15] for the triplets.
[b] $R_{(CH)}$ bond length was held constant at the GS equilibrium distance of 2.076 a_0.

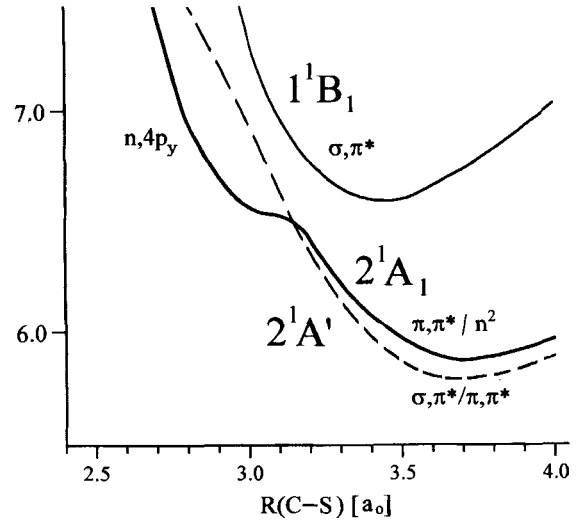

FIGURE 9. C — S stretch potentials of H_2CS showing that the potential of $\sigma, \pi^*/\pi, \pi^*$ at $\theta = 36.2°$ (dashed curve) is nearly parallel to the $\pi, \pi^*/n^2$ potential at $\theta = 0.0°$.

In the same article [13], calculated vibrational energies and oscillator strengths are given both for the $\pi, \pi^*/n, 4p_y$ *adiabatic* potential, similar to the π, π^*/Rydberg states discussed earlier for H_2CO, and for the *diabatic* $n, 4p_y$ potential. In both cases, the calculated energy for the 0–0 band (6.65 eV adiabatic, 6.56 eV diabatic) agrees well with the observed origin of the $n \rightarrow 4p_y$ system at 6.60 eV [20]. However, in the adiabatic case, two additional strong bands, at 6.82 (3_0^1) and 6.99 eV (3_0^2), are predicted, whereas in the diabatic case, higher bands have very low oscillator strengths. Unfortunately, the spectrum above 6.6 eV is poorly resolved, and, therefore, it cannot yet be determined which potential, diabatic or adiabatic, approaches reality more closely. Our experience with H_2CO would give a preference to the adiabatic results.

For H_2CS, spectra resulting from higher π, π^*/Rydberg potentials have not been investigated. A complication arises here due to the doubly excited n^0, π^{*2} state, whose C — S potential lies, as was mentioned earlier, between the two lowest $^1A_1$ Rydberg states and crosses them as well as π, π^*.

TABLE IV
Vibronic transition energies $\Delta E_0^{v'}$ (in eV) and oscillator lengths $f_0^{v'}$ for the 2^1A_1 $(\pi, \pi^*) \leftarrow \tilde{X}$ system in H_2CS.

v'	$\Delta E_0^{v'}$ calcd.[a]	$\Delta E_0^{v'}$ exptl.[b]	$f_0^{v'}$ calcd.[a]
0	5.821	—	4×10^{-7}
1	5.879	5.876	4×10^{-6}
2	5.949	5.927	2×10^{-5}
3	6.006	5.981	7×10^{-5}
4	6.065	6.036	2×10^{-4}
5	6.122	6.111	5×10^{-4}
6	6.177	6.138	9×10^{-4}
7	6.231	6.193	0.001
8	6.282	6.243	0.002
9	6.331	6.297	0.003

[a]Values from [13], assuming planar geometry.
[b]Estimated energies of band maxima from the spectrum of Moule et al. [19].

The Triplet π, π^* States of H_2CO and H_2CS

In Figure 10, the $^3A_1$ potential curves for the C — O stretch of H_2CO are shown. It is seen that the $^3(\pi, \pi^*)$ potential lies well below the Rydberg

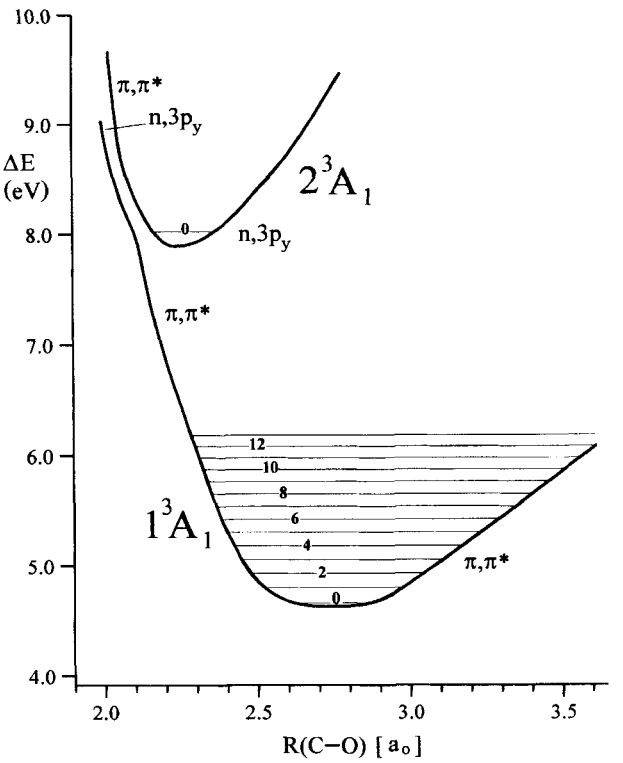

FIGURE 10. C — O stretch potentials of H_2CS for $^3A_1$ states of H_2CO, showing the location of π, π^* relative to $n, 3p_y$.

states, and the triplet $\pi \rightarrow \pi^*$ system should therefore be free of the Rydberg mixing which plagues its singlet counterpart. An electron-impact study by Taylor et al. [6] provided vibronic energies and intensities with which our calculated energies and Franck–Condon factors (based on the potential from Fig. 10) agree closely.

Contrary to the singlet π, π^* state, $^3(\pi, \pi^*)$ is nonplanar, as shown in the out-of-plane potentials in Figure 11. The calculated inversion barrier is 0.1 eV. The reason for the singlet being planar, and the triplet nonplanar, arises from the mixing of π, π^* with the closed-shell configuration n^2 in the singlet case, which is not possible for the triplet. Obviously, n^2 prefers planarity, whereas π, π^*, in conformity with the Mulliken–Walsh rules, prefers a nonplanar conformation. The optimized geometries and T_e's of $^3(\pi, \pi^*)$, $^3(\sigma, \pi^*)$, and $^3(n, 3p_y)$ are included in Table II. In contrast to the singlet case, σ, π^* lies well above π, π^*, and, therefore, mixing between these configurations is negligible.

The situation for the triplet π, π^* of H_2CS is similar to that of H_2CO. In the planar case, $1^3A_1(\pi, \pi^*)$ lies much lower than the Rydberg states, and $^3(\pi, \pi^*)$ is nonplanar with $\theta = 28°$, having an inversion barrier of 0.05 eV [14]. Its optimized geometry and T_e, as well as values for $^3(\sigma, \pi^*)$ and $^3(n, 4p_y)$, are given in Table III.

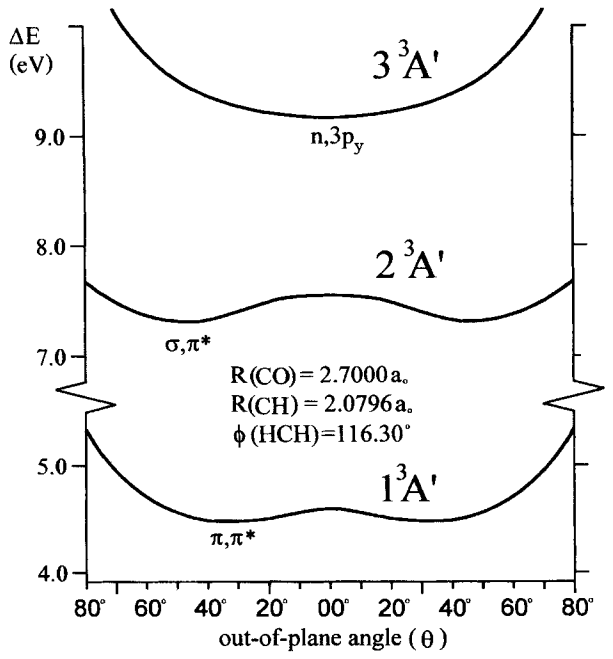

FIGURE 11. Out-of-plane potentials for $^3A'$ states of H_2CO, at $R_{CO} = 2.70\ a_0$.

Summary and Conclusion

In the absorption spectrum of formaldehyde, the $^1(\pi, \pi^*) \leftarrow \tilde{X}$ system is not seen directly, since the C — O stretch potential of π, π^* is repulsive and crosses all $^1A_1$ Rydberg potentials (as well as the ground-state potential). As a consequence, a series of avoided crossing minima are found which are bound on the left (smaller R_{CO}) by a section of the π, π^* potential, and on the right, by a Rydberg potential. Due to the fact that π, π^* and n, Rydberg states differ by a double excitation, their interaction is weak, as seen in the small energy difference between the states at the point of the avoided crossing, and usually the configuration change is very abrupt.

Due to such mixed π, π^*/Rydberg potentials, the high intensity of the π, π^* transition is transferred to Rydberg states within the same symmetry species, making them appear much more intense than they ought to be, and also shifting their positions in unexpected ways, resulting in unusual quantum defects. Using the C — O stretch mode, all strong and medium peaks of the absorption spectrum of H_2CO above 8 eV could, at least in principle, be explained in this way. Many details still need to be sorted out, such as non-Born–Oppenheimer interactions, which should be particularly important near the avoided crossings. The further crossing of π, π^* into the GS may explain the observed predissociation of Rydberg bands.

For thioformaldehyde, as for H_2CO, the $^1(\pi, \pi^*)$ potential crosses all Rydberg potentials as well as the ground-state potential. Since the lowest $^1A_1$ Rydberg state is crossed near its minimum the π, π^* system has higher Franck–Condon factors than in the case of H_2CO and becomes directly observable.

Complications are introduced by the out-of-plane motion. While $^1(\pi, \pi^*)$ of H_2CO has a local minimum for the planar conformation, there is only a low barrier of about 0.2 eV toward the nonplanar global $^1(\sigma, \pi^*)$ minimum, lying 0.35 eV below $^1(\pi, \pi^*)$. For H_2CS, the $^1(\pi, \pi^*)$ minimum that is seen in the R_{CS} potential curves for planar geometry becomes a saddle point when the out-of-plane motion is also taken into account. However, the $^1(\sigma, \pi^*)$ minimum lies only about 0.1 eV below the π, π^* minimum. Therefore, the observed "π, π^* bands" of H_2CS should better be called σ, π^* bands, according to the predominant

configuration of the global minimum. Due to the small energy difference between π, π^* and σ, π^*, and the fact that the C — S potential at the out-of-plane angle $\theta = 36.2°$, corresponding to the optimized value for σ, π^*, is nearly parallel to that at $\theta = 0°$, the distinction between $^1(\sigma, \pi^*)$ and $^1(\pi, \pi^*)$ for the C — S stretch is perhaps not so important. The very shallow potential of $2\,^1A'$ over two internal coordinates is expected to introduce some interesting features into the spectrum.

For the triplet π, π^* states of both H_2CO and H_2CS, the R_{CO} (R_{CS}) potential curves lie well below the $^3A_1$ Rydberg potentials. Therefore, the $^3(\pi, \pi^*)$ spectra should be observable and have, indeed, been seen for H_2CO. For both molecules, $^3(\pi, \pi^*)$ is nonplanar, with energy lowerings from the planar to the nonplanar conformation of 0.17 eV for H_2CO, and 0.07 eV for H_2CS. Again, one deals here with fairly shallow potentials.

For alkylated carbonyl compounds, such as acetaldehyde and acetone, as well as for many larger systems, the $^1(\pi, \pi^*)$ transition has also not been assigned, although, as in H_2CO, it may have been observed indirectly. Recent calculations on acetone [21] give R_{CO} potential curves very similar to those of H_2CO. On the other hand, substitutions of hydrogens by halogens raise the energy of Rydberg states relative to π, π^*, due to the stabilization of the n_0 orbital interacting with halogen lone pairs. According to calculations performed in this laboratory [22], the $^1(\pi, \pi^*)$ potentials of F_2CO, Cl_2CO, and Cl_2CS lie well below the Rydberg potentials.

In summary, the fact that the $^1(\pi, \pi^*)$ state has not been observed directly in the spectrum of formaldehyde and alkylated carbonyl compounds can be explained by the accidental and somewhat unfortunate positioning of the $^1(\pi, \pi^*)$ R_{CO}-potential relative to the $^1A_1$ Rydberg potentials. As a consequence, $^1(\pi, \pi^*)$ transfers its intensity to the Rydberg states, providing them with unusually high oscillator strengths and also changing the vibrational energy levels.

ACKNOWLEDGMENTS

This work was supported by the Natural Sciences and Engineering Research Council (NSERC) of Canada. We are grateful to Dr. P. Bruna for his contributions to the understanding of H_2CO and H_2CS and for many helpful discussions.

References

1. M. B. Robin, *Higher Excited States of Polyatomic Molecules* (Academic Press, New York, 1974), Vol. 2.
2. B. Niu, D. A. Shirley, Y. Bai, and E. Daymo, Chem. Phys. Lett. **201**, 212 (1993).
3. S. R. Langhoff, S. T. Elbert, C. F. Jackels, and E. R. Davidson, Chem. Phys. Lett. **29**, 247 (1974).
4. W. C. Price, J. Chem. Phys. **3**, 256 (1935).
5. P. Brint, J. P. Connerade, C. Mayhew, and K. Sommer, J. Chem. Soc., Faraday Trans. 2 **81**, 1643 (1985).
6. S. Taylor, D. G. Wilden, and J. Comer, J. Chem. Phys. **70**, 291 (1982).
7. M. R. J. Hachey, P. J. Bruna, and F. Grein, J. Chem. Soc., Faraday Trans. **90**, 683 (1994).
8. M. R. J. Hachey, P. J. Bruna, and F. Grein, J. Phys. Chem. **99**, 8050 (1995).
9. P. J. Bruna, M. R. J. Hachey, and F. Grein, J. Phys. Chem. **99**, 16576 (1995).
10. M. R. J. Hachey, P. J. Bruna, and F. Grein, J. Mol. Spectrosc. **176**, 375 (1996).
11. M. R. J. Hachey and F. Grein, Chem. Phys. Lett. **256**, 179 (1996).
12. M. R. J. Hachey, F. Grein, and R. P. Steer, Chem. Phys. Lett. **183**, 204 (1991).
13. M. R. J. Hachey and F. Grein, Can. J. Phys. **73**, 18 (1995).
14. M. R. J. Hachey and F. Grein, J. Mol. Spectrosc. **172**, 384 (1995).
15. M. R. J. Hachey and F. Grein, Chem. Phys. **197**, 61 (1995).
16. R. J. Buenker, S. D. Peyerimhoff, and W. Butscher, Mol. Phys. **35**, 771 (1978); R. J. Buenker, Int. J. Quantum Chem. **29**, 435 (1986); D. B. Knowles, J. R. Álvarez, G. Hirsch, and R. J. Buenker, J. Chem. Phys. **92**, 585 (1990), and references therein.
17. J. L. Duncan, Mol. Phys. **28**, 1177 (1974).
18. D. R. Johnson, F. X. Powell, and W. H. Kirchhoff, J. Mol. Spectrosc. **39**, 136 (1971).
19. C. R. Drury, J. Y. K. Lai, and D. C. Moule, Chem. Phys. Lett. **87**, 520 (1982).
20. C. R. Drury and D. C. Moule, J. Mol. Spectrosc. **92**, 469 (1982).
21. M. Merchán, B. O. Roos, R. McDiarmid, and X. Xing, J. Chem. Phys. **104**, 1791 (1996).
22. M. R. J. Hachey and F. Grein, to be submitted.